An Ensemble Method for Analyzing Spectral and Clinical Data of Patients with Skin Neoplasms

Ksenia E. Tomnikova* **and Irina A. Matveeva**
Samara National Research University, 34 Moskovskoye shosse, Samara 443086, Russian Federation
*e-mail: ksetomnikova@yandex.ru

Abstract. The work is devoted to the application of the ensemble method for the analysis of spectral and clinical data of patients with skin neoplasms. In vivo Raman spectra of skin neoplasms are used as spectral data. To identify the features reflecting the relative concentrations of skin components, the multivariate curve resolution method was used. In addition to spectral signs, clinical data on patients (anamnesis) were used. Ensemble models based on stacking have been developed for three classification cases: benign versus malignant neoplasms, malignant melanoma versus pigmented nevus, malignant melanoma versus pigmented nevus, and seborrheic keratosis. The the area under the Receiver Operating Characteristic (ROC) curve (ROC AUC) of the developed models ranges from 0.81 ± 0.06 to 0.85 ± 0.11, which confirms the effectiveness of the ensemble method and the anamnesis for the identification of skin neoplasms.

Keywords: skin neoplasms; Raman spectroscopy; multivariate curve resolution method; ensemble algorithm; stacking; medical history; clinical data.

Paper #9389 received 23 Oct 2025; revised manuscript received 22 Dec 2025; accepted for publication 22 Dec 2025; published online 30 Dec 2025. doi: 10.18287/JBPE25.11.040309.

1 Introduction

Skin neoplasms are one of the most common groups of diseases in the world [1]. Among them, there are benign neoplasms that are not life-threatening, as well as extremely malignant ones, for example, malignant melanoma. That is why accurate and rapid diagnosis of skin neoplasms is an urgent task of modern medicine [2].

The “gold standard” for the diagnosis of skin neoplasms is histological analysis. However, this method has a number of disadvantages, such as invasiveness and the length of waiting for results. Optical diagnostic methods, in particular, Raman spectroscopy, are gaining increasing popularity [2]. Compared to histological analysis, Raman spectroscopy is faster and cheaper. In addition, Raman spectroscopy can make the diagnosis of skin diseases completely non-invasive.

Various studies demonstrate that Raman spectroscopy can be used to make diagnostic decisions, that is, to determine the disease or type of neoplasm [1]. However, despite advances in technical equipment, the analysis of experimental Raman spectra remains a difficult task. The reason for this is that the Raman spectra of light contain a large amount of information about all the chemicals contained in the skin, and may also contain spurious signals caused by the optical system [3].

In this regard, an urgent task is to find a new method for interpreting the Raman spectra of the skin.

As part of the research, the task of classifying Raman skin spectra was performed using a number of machine learning algorithms. The multidimensional curve resolution (MCR) method was used to reduce the initial spectral data. A comparative analysis of the classification efficiency was carried out on sets of features formed with a different number of decomposition components: 8, 10, 15 and 30. It was found that the highest classification accuracy is achieved when using a set of 30 components, which indicates a more complete description of the spectral variability of biological samples [4–6].

It is assumed that taking into account the clinical data of patients (that is, their medical history) provides additional information for a more accurate classification and interpretation of spectra [7].

Medical history plays an important role in the diagnosis of skin diseases. Information about past illnesses, allergies, heredity, and lifestyle helps the doctor create a complete picture of the patient’s

condition. To make a correct diagnosis, it is necessary to know when the disease began, how it developed, and what symptoms are bothering the patient. In addition, it is necessary to take into account the presence of concomitant diseases, place of residence and risk factors in the workplace [8].

Taking an anamnesis is the first step in making a diagnosis. It is based on finding out: the duration of the disease; the severity of its onset; localization; the prevalence of the process; symptoms of the disease; family history; profession; previous treatment.

The purpose of collecting medical history is also to clarify the etiological factors contributing to the occurrence of dermatosis. By tradition, the medical history begins to be collected before the general examination.

An important part of the diagnostic process is clarifying the life history. When collecting it, one should strive to identify possible etiological factors, including: alcohol consumption; taking medications; conditions of professional activity; peculiarities of everyday life; family history.

When collecting a life history, information about past illnesses is important.

Skin diseases are often a manifestation of internal pathology. Thus, diabetes mellitus can cause candidiasis of the skin, and malignant neoplasms of internal organs can metastasize to the skin [9].

The course of some skin diseases depends on the season [10]. Diseases associated with the adverse effects of ultraviolet rays (photodermatoses) are more common in spring and summer. Erythema multiforme and pink lichen − in spring and autumn. Dermatoses caused by impaired capillary circulation (cold urticaria) are common in the cold season.

Thus, the integration of clinical and spectral data is not just a technical improvement, but a methodological necessity for the transfer of spectroscopic methods from the research plane into real clinical practice.

The vast majority of research devoted specifically to spectral methods focuses exclusively on spectra. If clinical data is used, it is at the stage of sample formation or for post-analytical interpretation of the results, but it is not directly integrated into the model at the feature level [11−14].

Thus, the novelty of our method lies in the purposeful and systematic combination of two modalities − biochemical (Raman spectra) and phenotypic (clinical data) − into a single analytical model. This allows us to create a model that simultaneously takes into account both the molecular composition of the tissue and the individual characteristics of the patient, which leads to the creation of a more reliable and clinically applicable decision support tool.

Based on the above, the aim of the work was to implement an ensemble algorithm for the identification of skin growths, taking into account spectral data and the patient’s medical history.

2 Methods and Materials

2.1 Raman Spectra

The Raman spectra of neoplasms were recorded using a portable spectroscopic setup with a spectral resolution of 0.2 nm in the range from 860 to 922 nm with a signal accumulation time of 60 seconds when excited at a wavelength of 785 nm.

The spectra were preprocessed, including cropping in the range from 860 to 920 nm, baseline removal, and smoothing using the Savitsky-Golay method.

The *in vivo* study was conducted at the Samara Regional Clinical Oncology Dispensary. More than 500 patients participated in the study. For each patient, the spectrum from the skin area with the disease was recorded. In addition to the Raman spectra, information about the actual diagnoses for each patient was obtained. These diagnoses were made by doctors of the Samara Regional Clinical Oncological Dispensary based on the results of histological analysis. Table 1 shows information about the set of registered Raman spectra.

Table 1 Raman spectra.

Nosology	Number of registered Raman spectra
Dermatofibroma	26
Hemangioma	40
Sebrrheic keratosis	113
Basal cell carcinoma	122
Squamous cell carcinoma	12
Malignant melanoma	70
Pigmented nevus	170
Papilloma	62

2.2 Clinical Data

It can be argued that the clinical picture is extremely important for making a correct diagnosis of skin diseases. Therefore, in addition to spectral data, clinical data and patient anamnesis were collected. The study involved 178 men and 437 women.

At the first appointment, the oncologist collected the patient's medical history and potential risk factors for skin cancer: gender, age, place of residence, genetic predisposition, eye color, harmful profession, indoor work, concomitant diseases, the presence of skin diseases in the past, the presence of sunburn, tumor localization, age spot size, height spots, bleeding, dropouts, and localization. All data has been encoded (Table 2).

All 15 risk factors were later used as classification parameters.

Table 2 Encoding of the collected clinical data.

Sign	Encoding
Gender	0 – female 1 – male
Age	number of years from 20 to 88
Place of residence	0 – city 1 – village
Genetic predisposition	0 – no 1 – Father and mother 2 – Brother and sister 3 – Grandma and Grandpa 4 – distant relatives
Eye color	1 – gray 2 – blue 3 – green 4 – brown
Harmfulness of the profession	0 – no 1 – yes
Working indoors for more than 15 years	0 – yes 1 – no
Concomitant diseases	0 – no 1 – malignant tumors 2 – cardiovascular diseases 3 – diabetes mellitus 4 – thyroid diseases
The presence of skin diseases in the past	0 – no 1 – benign neoplasms 2 – malignant neoplasms
The presence of sunburn	0 –never been 1 – has been 1-2 times 2 – occur quite often
Localization of the tumor	1– head and neck 2 – the torso 3 – upper limb 4 – lower limb
The size of the pigment spot	1 — from 0 to 5 mm 2 — from 6 to 20 mm 3 — 21 mm
Spot growth	0 – yes 1 – no
Bleeding	0 – yes 1 – no
The appearance of dropouts and localization	0 – yes 1 – no

2.3 The Multivariate Curve Resolution Method

To reduce the amount of spectral data, the multidimensional curve resolution (MCR) method was applied. It is a method of analyzing multidimensional data that allows you to separate complex mixtures into their constituent components. It is based on the use of linear algebra to extract information about components from multidimensional data.

Each pure component has its own spectrum, which can be represented as a column vector si of dimension *J*, where *J* is the number of values in each spectrum (corresponding to the number of wavelengths or wave numbers).

If you mix the components into one mixture and remove its spectrum, then the resulting spectrum will simply be a linear combination of the spectra of the pure components. This can be expressed by the equation:

$$D = CS^T, \quad (1)$$

where *C* is the matrix of concentrations of pure components in the mixture; *S* is the matrix of spectra of pure components.

The task of MCR methods is to find the matrices *C* and *S*, knowing *D*. This is not a trivial task, since the specified expression does not have a single solution.

The main advantage of MCR analysis is the ability to physically interpret the components into which the original Raman spectra are divided. The analysis results in:

• the spectra of the substances that make up the sample;

• their contribution to the Raman spectrum (which is directly related to the actual concentrations of substances) [15, 16].

In addition, unlike, for example, the methods of Principal Component Analysis (PCA) and Partial Least Squares Discriminant Analysis (PLS AD), this method is more resistant to outliers in the data.

Some researchers divide such spectra into 8−10 components to identify specific substances [17]. Such a goal was not set in this work: it was important to preserve the maximum possible amount of valuable information for classifying the Raman spectra of the skin.

After completing the MCR analysis, compressed spectral data is obtained in the form of 30 components and their concentrations in each sample of biological tissue. The data on the concentrations of the obtained substances are further used as classification criteria. The MCR ALS GUI v4c program developed by Dr. Andras Gorjas (Sweden) was used to implement the MCR analysis [18].

Basically, the resulting components are different mixtures of lipids and proteins. But there are also those that are purer substances, some of them are shown in the Fig. 1. Components 1, 4 have identical shapes, they have peaks at 1161 cm^{-1} and 1182 cm^{-1}, respectively, and are ceramides. Components 6 and 9 correspond to the optical contribution of the system. In component 7, the most intense peaks are at 1450 and 1662 cm^{-1}, these peaks correspond to collagen. In component 17, the highest peak is at 1652 cm^{-1}, which corresponds to the peak in the water spectrum. Component 24 contains 1654 cm^{-1} water, 1372 and 1564 cm^{-1} melanin, and various proteins. In component 30, the most pronounced peaks at 1290, 1450, and 1657 cm^{-1} correspond to C-H bending proteins and may be due to keratin, collagen, and elastin. In addition, the peak at 1450 cm^{-1} may also correspond to the contribution of urocanoic acid [19].

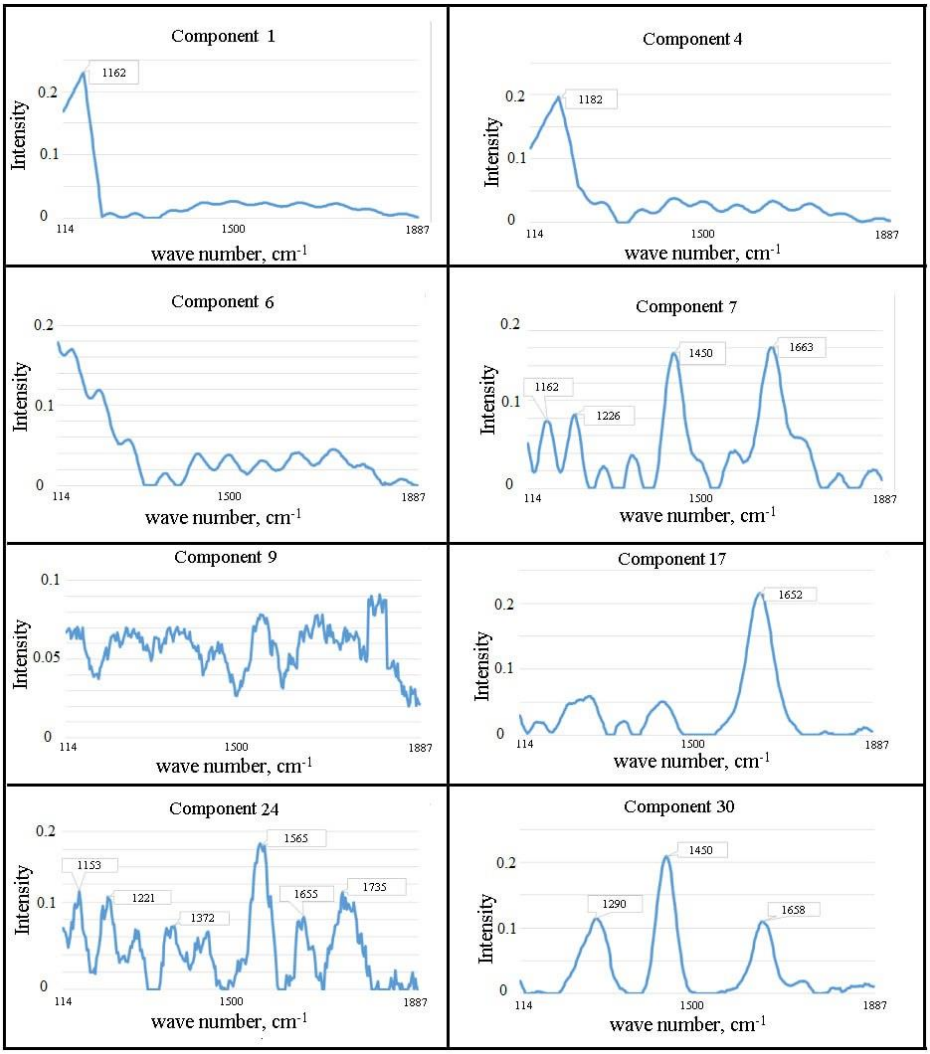

Fig. 1 Spectra of some of the obtained components.

The choice of exactly 30 components was not accidental. Several additional studies were conducted to determine the optimal number of components in order to reduce the amount of data without losing valuable information [4, 5].

2.4 The Ensemble Algorithm

The ensemble algorithm was developed for three cases:

- benign neoplasms versus malignant neoplasms (case 1);
- malignant melanoma versus pigmented nevus (case 2);
- malignant melanoma versus pigmented nevus and seborrheic keratosis (case 3).

The paper examines the application of an ensemble algorithm that takes into account the solutions of several independently operating machine learning algorithms: random forest, gradient boosting and multilayer perceptron. The algorithms were implemented in the Python programming language using the scikit-learn and LightGBM libraries.

First, a study was conducted to find the optimal hyperparameters for each individual model included in the ensemble (random forest, gradient boosting, and multilayer perceptron). The Grid Search method was used.

For a random forest, such hyperparameters were selected as n_estimators – the number of “trees”, max_depth – the maximum depth of the “trees”, min_samples_split – the minimum number of objects required to split a node, min_samples_leaf – the minimum number of objects in the “leaves”. The values of the obtained hyperparameters for a random forest are shown in Table 3.

Table 3 Hyperparameters of a random forest for different cases.

Hyperparameter	Case 1	Case 2	Case 3
n_estimators	100	100	775
max_depth	25	13	25
min_samples_split	2	26	2
min_samples_leaf	2	2	2

Table 4 Hyperparameters of gradient boosting for different cases.

Hyperparameter	Case 1	Case 2	Case 3
n_estimators	100	1050	100
max_depth	1	1	1
num_leaves	2	2	2
learning_rate	0.0001	0.1	0.0001

Table 5 Hyperparameters of a multilayer perceptron for different cases.

Hyperparameter	Case 1	Case 2	Case 3
hidden_layer_sizes	100, 50	100	100
activation	logistic	logistic	logistic
max_iter	400	300	300
solver	sgd	adam	sgd

Such hyperparameters as n_estimators, the number of "trees", max_depth, the maximum depth of the "trees", num_leaves, the number of "leaves" in the "tree", and learning_rate, the learning rate of the model, were chosen as the hyperparameters of gradient boosting. The results of executing the GridSearch command for gradient boosting are shown in Table 4.

To develop the multilayer, hyperparameters were used: hidden_layer_sizes – the number of neurons in each hidden layer, activation – the activation function for hidden layers, max_iter – the maximum number of training iterations, solver – an algorithm for optimizing weights. Table 5 shows the hyperparameters found for a multilayer perceptron.

Next, models with optimal hyperparameters were combined into an ensemble using the stacking method, when the predicted values of the basic individual models are used as input data to the overall meta-model. Logistic regression was chosen as a meta-model.

3 Results and Discussion

To prove the effectiveness of the ensemble algorithm models using patient clinical data, Figs. 2, 3 and 4 show ROC curves for different classification cases, where only the concentrations of the substances obtained and a data set with concentrations of substances and clinical data of patients were used as parameters.

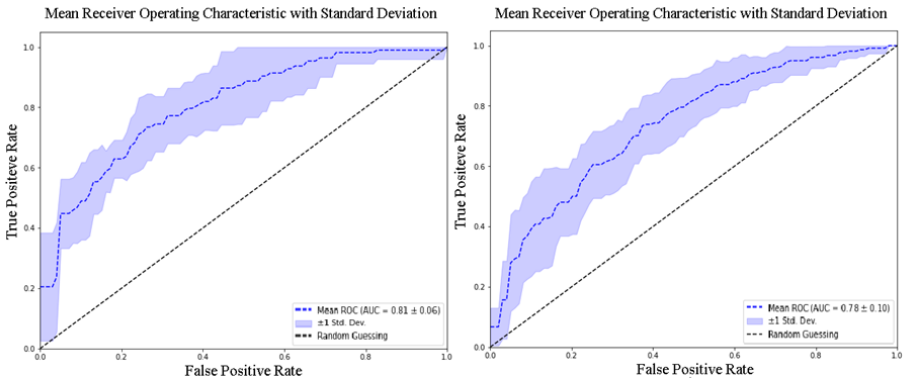

(a) (b)

Fig. 2 ROC curves for the case of benign versus malignant neoplasms: (a) an ensemble algorithm with clinical data, (b) an ensemble algorithm without clinical data.

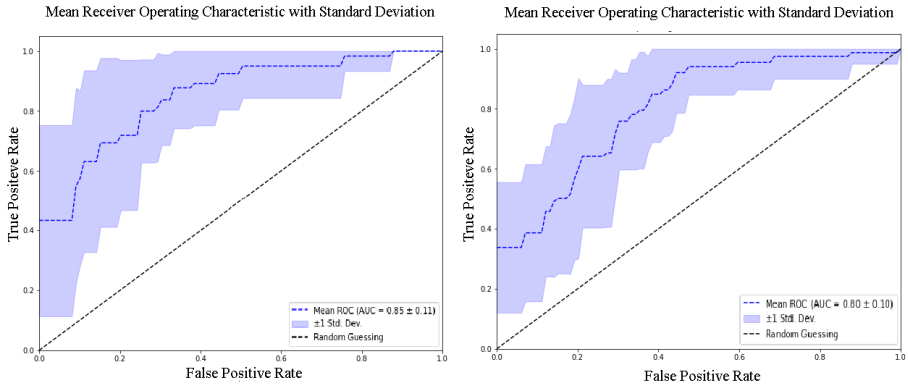

(a) (b)

Fig. 3 ROC curves for malignant melanoma versus pigmented nevus: (a) an ensemble algorithm with clinical data, (b) an ensemble algorithm without clinical data.

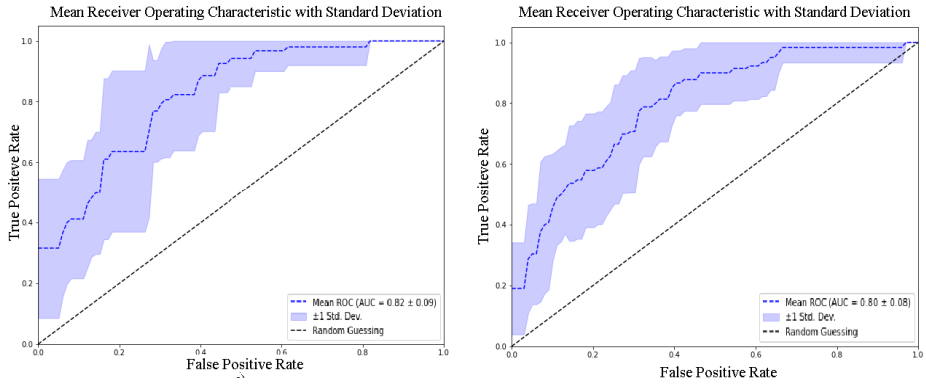

(a) (b)

Fig. 4 ROC curves for the case of malignant melanoma versus pigmented nevus and seborrheic keratosis: (a) an ensemble algorithm with clinical data, (b) an ensemble algorithm without clinical data.

Table 6 Metrics of classification models.

The classification case	ROC AUC (no medical history)	ROC AUC (with medical history)
Benign neoplasms vs. malignant neoplasms	0.78±0.10	0.81±0.06
Malignant melanoma vs. pigmented nevus	0.80±0.10	0.85±0.11
Malignant melanoma vs. (pigmented nevus + seborrheic keratosis)	0.80±0.08	0.82±0.09

Table 6 shows the average values of ROC AUC with the standard deviation calculated for all folds. One column contains information for models where only spectral information about the neoplasm was used as signs, and the other column takes into account both spectral signs and clinical patient data (anamnesis).

The quality of skin cancer diagnosis by visual examination largely depends on the level of qualification and professional experience of the doctor. For example, a doctor correctly identifies malignant melanoma only in 40−80% of cases (depending on qualifications) [20, 21].

Based on this, the ROC AUC threshold of 0.8 was chosen for a decent primary diagnosis of skin diseases by the method being developed.

The development results fully satisfy the task. In all cases, the ROC AUC exceeds the threshold of 0.8.

In the case of benign neoplasms against malignant ones, the ROC AUC increased by 0.03, from 0.78 ± 0.10 to 0.81 ± 0.06. The ROC AUC for the case of malignant melanoma against pigmented nevus was 0.85 ± 0.1, increased by 0.05 compared with the ensemble without clinical data, and in the case of malignant melanoma against pigmented nevus and seborrheic keratosis increased by 0.02 and it was 0.82 ± 0.09.

To understand whether the increase in ROC AUC is statistically significant, a paired *t*-test was performed. The *p*-value for benign versus malignant neoplasms was 0.279, for malignant melanoma versus pigmented nevus – 0.165, and for malignant melanoma versus pigmented nevus and seborrheic keratosis – 0.477. Statistical analysis shows that the observed improvements in ROC AUC with the addition of clinical data are not statistically significant at the generally accepted level of $p < 0.05$, although it shows an improvement trend.

It can be seen from this study that the data on the relative concentrations in the studied samples is sufficient for automated diagnostics. However, interpretability of data is important for medicine, so clinical data can be included in the model so that the model makes predictions not only based on spectral data, but also on the basis of signs that the doctor understands – clinical data. That is why both approaches should be used to identify the Raman spectra of the skin.

In addition to ROC AUC, specificity and sensitivity were calculated for the models, and their values are shown in the Table 7.

Table 7 Specificity and sensitivity of the model for different cases.

	no medical history		
	Case 1	Case 2	Case 3
Specificity	0.55	0.52	0.38
Sensitivity	0.86	0.82	0.88
	with medical history		
	Case 1	Case 2	Case 3
Specificity	0.60	0.57	0.43
Sensitivity	0.81	0.82	0.87

The addition of clinical data to the ensemble classification model of Raman skin spectra allowed us to create a more balanced diagnostic tool with significantly increased specificity while maintaining very high sensitivity. This shows that combining spectroscopy data and clinical information gives a better result than each method individually.

It can be said that the method of Raman spectroscopy is comparable to the diagnosis by doctors during dermotoscopic examination. Thus, in the study by Haenssle et al. [20], the average sensitivity and specificity of 58 dermatologists for the classification of 100 skin lesions was 86.6% (±9.3%) and 71.3% (±11.2%), which corresponds to the diagnostic accuracy (the proportion of correctly determined diagnoses) of 79% (±0.06%).

4 Conclusion

As a result of the work, an ensemble stacking-based method was developed for the classification of Raman spectra of skin neoplasms using clinical patient data.

In addition to the high accuracy of the classification of skin diseases, due to the use of the MCR analysis method to reduce the amount of data, the developed algorithm makes it possible to identify real chemicals in the test sample.

In each case, the accuracy of the classification is comparable to the accuracy of the identification of the disease by an experienced oncologist.

The considered method of Raman spectroscopy in combination with intelligent analysis and taking into account the medical history of patients can be used for population screening as a fast and fairly accurate method of analyzing skin neoplasms. It can also be implemented in hospitals where there is a lack of highly qualified personnel and technical equipment.

Disclosures

All authors declare that there is no conflict of interest in this paper.

References

1. J. Ferlay, M. Colombet, I. Soerjomataram, D. M. Parkin, M. Piñeros, A. Znaor, and F. Bray, "Cancer statistics for the year 2020: An overview," International Journal of Cancer 149(4), 778–789 (2021).
2. O. I. Kaganov, I. G. Loginova, A. A. Moryatov, S. V. Kozlov, A. E. Orlov, I. A. Bratchenko, and B. B. Dzhuraev, "Raman spectroscopy in optical non-invasive diagnostics of skin neoplasms," Creative Surgery and Oncology 14(2), 136–141 (2024). [in Russian]
3. I. A. Bratchenko, L. A. Bratchenko, A. A. Moryatov, Y. A. Khristoforova, D. N. Artemyev, O. O. Myakinin, A. E. Orlov, S. V. Kozlov, and V. P. Zakharov, "In vivo diagnosis of skin cancer with a portable Raman spectroscopic device," Experimental Dermatology 30(5), 652–663 (2021).
4. K. Tomnikova, I. Matveeva, "Application of multivariate curve resolution analysis and multilayer perceptron for classification of raman spectra of the skin," 2024 Intelligent Technologies and Electronic Devices in Vehicle and Road Transport Complex (IEEE, 2024), 1–5 (2024).
5. K. E. Tomnikova, I. A. Matveeva, "Investigation of spectral features for the classification of Raman skin spectra by the random forest method," XXII All-Russian Samara Youth Competition-Conference on Optics, Laser Physics and Plasma Physics, 213–214 (2024).
6. K. E. Tomnikova, I. A. Matveeva, "Machine learning methods for classifying raman scattering spectra of the skin," X International Conference on Information Technology and Nanotechnology (ITNT), 1–4 (2024).
7. Y. Khristoforova, I. Bratchenko, L. Bratchenko, A. Moryatov, S. Kozlov, O. Kaganov, and V. Zakharov, "Combination of optical biopsy with patient data for improvement of skin tumor identification," Diagnostics 12(10), 2503 (2022).
8. A. A. Kubanov, M. A. Kaspirovich, L. Y. Melekhina, M. M. Butareva, and A. B. Rubtsov, "Informatization of medical organizations of dermatovenerological profile. Modern statistical accounting requirements," Vestnik Dermatologii i Venerologii 88(1), 6–12 (2012).
9. S. Shahabudin, N. S. Azmi, M. N. Lani, M. Mukhtar, and M. S. Hossain, "*Candida albicans* skin infection in diabetic patients: An updated review of pathogenesis and management," Mycoses 67(6), e13753 (2024).
10. P. Lehmann, "Photodermatoses," Braun-Falco's Dermatology, W. H. C. Burgdorf, G. Plewig, H. H. Wolff, M. Landthaler, and O. Braun-Falco (Eds.), Springer Berlin Heidelberg, 573–597 (2009).
11. H. Lui, J. Zhao, D. McLean, and H. Zeng, "Real-time Raman spectroscopy for in vivo skin cancer diagnosis," Cancer Research 72(10), 2491–2500 (2012).
12. M. Gniadecka, P. A. Philipsen, S. Wessel, R. Gniadecki, H. C. Wulf, S. Sigurdsson, O. F. Nielsen, D. H. Christensen, J. Hercogova, K. Rossen, H. K. Thomsen, and L. K. Hansen, "Melanoma diagnosis by raman spectroscopy and neural networks: structure alterations in proteins and lipids in intact cancer tissue," Journal of Investigative Dermatology 122(2), 443–449 (2004).
13. P. Tschandl, C. Rinner, Z. Apalla, G. Argenziano, N. Codella, A. Halpern, M. Janda, A. Lallas, C. Longo, J. Malvehy, J. Paoli, S. Puig, C. Rosendahl, H. P. Soyer, I. Zalaudek, and H. Kittler, "Human–computer collaboration for skin cancer recognition," Nature Medicine 26(8), 1229–1234 (2020).
14. [14] E. Borisova, P. Pavlova, E. Pavlova, P. Troyanova, and L. Avramov, "Optical biopsy of human skin—A tool for cutaneous tumours' diagnosis," International Journal Bioautomation 16(1), 53–72 (2012).

15. J. Felten, H. Hall, J. Jaumot, R. Tauler, A. De Juan, and A. Gorzsás, "Vibrational spectroscopic image analysis of biological material using multivariate curve resolution–alternating least squares (MCR-ALS)," Nature Protocols 10(2), 217–240 (2015).
16. I. A. Matveeva, A. I. Komlev, O. I. Kaganov, A. A. Moryatov, and V. P. Zakharov, "Multidimensional analysis of dermoscopic images and spectral information for the diagnosis of skin tumors," Journal of Biomedical Photonics & Engineering 10(1), 010307 (2024).
17. I. Matveeva, I. Bratchenko, Y. Khristoforova, L. Bratchenko, A. Moryatov, S. Kozlov, O. Kaganov, and V. Zakharov, "Multivariate curve resolution alternating least squares analysis of in vivo skin raman spectra," Sensors 22(24), 9588 (2022).
18. A. Gorzsás, "User Manual MCR-ALS GUI v4c," Vibrational Spectroscopy Core Facility, Department of Chemistry, Umeå University, SE-90187 Umeå, Sweden (2016).
19. X. Feng, A. J. Moy, H. T. M. Nguyen, J. Zhang, M. C. Fox, K. R. Sebastian, J. S. Reichenberg, M. K. Markey, and J. W. Tunnell, "Raman active components of skin cancer," Biomedical Optics Express 8(6), 2835 (2017).
20. H. A. Haenssle, C. Fink, R. Schneiderbauer, F. Toberer, T. Buhl, A. Blum, A. Kalloo, A. B. H. Hassen, L. Thomas, A. Enk, L. Uhlmann, C. Alt, M. Arenbergerova, R. Bakos, A. Baltzer, I. Bertlich, A. Blum, T. Bokor-Billmann, J. Bowling, N. Braghiroli, R. Braun, K. Buder-Bakhaya, T. Buhl, H. Cabo, L. Cabrijan, N. Cevic, A. Classen, D. Deltgen, C. Fink, I. Georgieva, L.-E. Hakim-Meibodi, S. Hanner, F. Hartmann, J. Hartmann, G. Haus, E. Hoxha, R. Karls, H. Koga, J. Kreusch, A. Lallas, P. Majenka, A. Marghoob, C. Massone, L. Mekokishvili, D. Mestel, V. Meyer, A. Neuberger, K. Nielsen, M. Oliviero, R. Pampena, J. Paoli, E. Pawlik, B. Rao, A. Rendon, T. Russo, A. Sadek, K. Samhaber, R. Schneiderbauer, A. Schweizer, F. Toberer, L. Trennheuser, L. Vlahova, A. Wald, J. Winkler, P. Wölbing, and I. Zalaudek, "Man against machine: diagnostic performance of a deep learning convolutional neural network for dermoscopic melanoma recognition in comparison to 58 dermatologists," Annals of Oncology 29(8), 1836–1842 (2018).
21. N. S. Eikje, K. Aizawa, and Y. Ozaki, "Vibrational spectroscopy for molecular characterisation and diagnosis of benign, premalignant and malignant skin tumours," Biotechnology Annual Review 11, 191–225 (2005).